

# Volume and surface contributions to the nuclear symmetry energy within the coherent density fluctuation model

A. N. Antonov,<sup>1</sup> M. K. Gaidarov,<sup>1</sup> P. Sarriguren,<sup>2</sup> and E. Moya de Guerra<sup>3</sup>

<sup>1</sup>*Institute for Nuclear Research and Nuclear Energy, Bulgarian Academy of Sciences, Sofia 1784, Bulgaria*

<sup>2</sup>*Instituto de Estructura de la Materia, IEM-CSIC, Serrano 123, E-28006 Madrid, Spain*

<sup>3</sup>*Grupo de Física Nuclear, Departamento de Física Atómica, Molecular y Nuclear, Facultad de Ciencias Físicas, Unidad Asociada UCM-CSIC(IEM), Universidad Complutense de Madrid, E-28040 Madrid, Spain*

(Received 28 January 2016; revised manuscript received 26 May 2016; published 22 July 2016)

The volume and surface components of the nuclear symmetry energy (NSE) and their ratio are calculated within the coherent density fluctuation model (CDFM). The estimations use the results of the model for the NSE in finite nuclei based on the Brueckner energy-density functional for nuclear matter. In addition, we present results for the NSE and its volume and surface contributions obtained by using the Skyrme energy-density functional. The CDFM weight function is obtained using the proton and neutron densities from the self-consistent HF+BCS method with Skyrme interactions. We present and discuss the values of the volume and surface contributions to the NSE and their ratio obtained for the Ni, Sn, and Pb isotopic chains, studying their isotopic sensitivity. The results are compared with estimations of other approaches which have used available experimental data on binding energies, neutron-skin thicknesses, excitation energies to isobaric analog states (IAS), and also with results of other theoretical methods.

DOI: [10.1103/PhysRevC.94.014319](https://doi.org/10.1103/PhysRevC.94.014319)

## I. INTRODUCTION

One of the most exciting topics of research in nuclear physics is currently the nuclear matter symmetry energy that essentially characterizes the isospin-dependent part of the equation of state of asymmetric nuclear matter (ANM) [1–4]. A natural and important way to learn more about the NSE is the transition from ANM to finite nuclei. Experimentally, the NSE is not a directly measurable quantity and is extracted indirectly from observables that are related to it (see, e.g., the review [5]). A sensitive probe of the NSE is the neutron-skin thickness of nuclei, although its precise measurement is difficult to be done. At present, the latter is derived from pigmy dipole resonance measurements [6], data on antiprotonic atoms [1], giant resonances, nuclear reactions, parity-violating asymmetry [7,8], and others. Correlations of the neutron-skin thickness in finite nuclei with various symmetry energy parameters are considered in Ref. [9]. A wide range of works (e.g., [10–14]) are devoted to studies of the density dependence of the symmetry energy in uniform matter.

The symmetry energy of finite nuclei at saturation density has been often extracted by fitting ground state masses with various versions of the liquid-drop mass formula within the liquid-drop models [15–17], and also within other approaches, such as the random phase approximation based on the Hartree-Fock (HF) approach [18], effective Lagrangians with density-dependent meson-nucleon vertex functions [19], the energy density functional (EDF) of the Skyrme force [20–22], relativistic nucleon-nucleon (NN) interactions [23,24], and others. In our previous works [25,26] the symmetry energy has been studied in a wide range of spherical and deformed nuclei, on the basis of the Brueckner EDF [27,28]. In these works the transition from the properties of nuclear matter to those of finite nuclei has been made using the coherent density fluctuation model [29,30]. The latter is a natural extension

of the Fermi-gas model based on the generator coordinate method [30,31] and includes long-range NN correlations of collective type. The numerous applications of the CDFM to analyses of characteristics of the nuclear structure and reactions can be seen, e.g., in Refs. [25,30]. In [25] the study of the correlation between the thickness of the neutron skin in finite nuclei and the NSE for the isotopic chains of even-even Ni ( $A = 74\text{--}84$ ), Sn ( $A = 124\text{--}152$ ), and Pb ( $A = 206\text{--}214$ ) nuclei, as well as the neutron pressure and the asymmetric compressibility for these nuclei, have been presented. The calculations have been based on the deformed self-consistent mean-field HF+BCS method [32,33], using the CDFM and the Brueckner EDF. The same approaches have been used in Ref. [26] for the calculations of the mentioned quantities of deformed neutron-rich even-even nuclei, such as Kr ( $A = 82\text{--}120$ ) and Sm ( $A = 140\text{--}156$ ) isotopes.

In 1947 Feenberg [34] pointed out that the surface energy should contain a symmetry energy contribution as a consequence of the failure of nuclear saturation at the edge of the nucleus and that the volume saturation energy also has a symmetry energy term. Cameron in 1957 [35] (see also Bethe [36]) suggested a revised mass formula in which the volume energy was expressed as a sum of two contributions: the volume saturation energy proportional to the mass number  $A$  and a volume symmetry energy assumed proportional to  $(A - 2Z)^2/A$ . In 1958 Green [37] estimated the values of the volume and surface components of the corresponding contributions to the symmetry energy. Myers and Swiatecki in 1966 [15] admitted that the ratio between the mentioned coefficients must be equal to the ratio between the surface and volume coefficients of the corresponding components of the mass formula. In Ref. [38] Warda *et al.* studied the bulk and the surface nature of the formation of the neutron skin in the isotopic chains of Sn and Pb, a concept that can be applied when analyzing the experimental data. In Ref. [39] the same

authors showed the role of the stiffness of the NSE on the origin of the neutron-skin thickness in  $^{208}\text{Pb}$ , the latter being decomposed into bulk and surface components. In Ref. [40] it was demonstrated by Danielewicz that the ratio of the volume to surface symmetry energy is closely related to the neutron-skin thickness (see also Refs. [41–48]). Discussions on the correlation between the bulk and surface symmetry energy are given also, e.g., in Refs. [49–53]. It was shown in [54] by Lee and Mekjian by calculations of the thermal nuclear properties that the surface symmetry-energy term is more sensitive to the temperature than the volume energy term. In Ref. [55] Agrawal *et al.* pointed out that, contrary to the case of the infinite nuclear matter, a substantial change in the symmetry energy coefficients is observed for finite nuclei with temperature.

In the present work we investigate the volume and surface contributions to the NSE within the CDFM. We use our results for NSE obtained using Brueckner EDF in Refs. [25,26,56], as well as the considerations of this subject mentioned above (e.g., [34–53]). The present calculations are performed using both Brueckner and, in addition, Skyrme energy-density functionals. The results are compared with those of other theoretical methods and with corresponding experimental data obtained from analyses of different nuclear quantities, such as binding energies, neutron-skin thicknesses, excitation energies to IAS, and others.

The structure of this paper is the following. In Sec. II we present the main relationships for the NSE and its volume and surface components that we use in our study. Section III contains the CDFM formalism that provides a way to calculate the mentioned quantities. There we also present the numerical results and discussions. The main conclusions of the study are given in Sec. IV.

## II. RELATIONSHIPS CONCERNING THE VOLUME AND SURFACE CONTRIBUTIONS TO NUCLEAR SYMMETRY ENERGY

The mass formula can be written in the form (e.g., Ref. [36])

$$E = -c_1 A + c_2 A^{2/3} + c_3' \frac{(N-Z)^2}{A} + \text{Coulomb term} + \text{shell corrections} \quad (1)$$

The first three terms in the right-hand side of Eq. (1) correspond to the volume, surface, and symmetry components of the energy. As mentioned in the Introduction, the symmetry energy has volume and surface contributions. Then, the third term in Eq. (1) has to be replaced by (see, e.g., [36])

$$\frac{(N-Z)^2}{A} (c_3 - c_4 A^{-1/3}). \quad (2)$$

Estimations of the coefficients  $c_3$  and  $c_4$  have been given in Ref. [37], but due to the substantial shell corrections there remained problems obtaining their values. In Ref. [15] it was admitted that the ratio  $c_4/c_3$  can be taken to be equal to the ratio  $c_2/c_1$  of the coefficients of the surface to volume components

of the energy (see also [36]):

$$\frac{c_4}{c_3} = \frac{c_2}{c_1} = \chi. \quad (3)$$

In the work of Myers and Swiatecki [15] the value of  $\chi$  is estimated to be 1.1838, while it is given to be 1.14 by Bethe in Ref. [36].

The expression for the energy per particle has the form

$$\bar{E} = \frac{E}{A} = -c_1 + c_2 \frac{1}{A^{1/3}} + c_3' \left( \frac{N-Z}{A} \right)^2 + \frac{1}{A} [\text{Coulomb term} + \text{shell corrections}]. \quad (4)$$

By definition the NSE coefficient is

$$s = \frac{1}{2} \frac{\partial^2 \bar{E}}{\partial \alpha^2} \Big|_{\alpha=0}, \quad (5)$$

where

$$\alpha \equiv \frac{N-Z}{A}. \quad (6)$$

Then it follows from Eqs. (5), (2), and (3) that

$$s = c_3' = c_3 - \frac{c_4}{A^{1/3}} = c_3 \left( 1 - \frac{\chi}{A^{1/3}} \right) \quad (7)$$

and

$$c_3 = \frac{s}{1 - \frac{\chi}{A^{1/3}}}, \quad c_4 = \chi \left( \frac{s}{1 - \frac{\chi}{A^{1/3}}} \right). \quad (8)$$

In modern times Danielewicz *et al.* (see, e.g., [40,41,48,50] and references therein) proposed the following expression for the symmetry energy:

$$E_{\text{sym}} = \frac{a_a(A)}{A} (N-Z)^2, \quad (9)$$

where the  $A$ -dependent coefficient  $a_a(A)$  is expressed by means of the volume ( $a_A^V$ ) and surface ( $a_A^S$ ) coefficients in the form

$$a_a(A) = \frac{a_A^V}{[1 + A^{-1/3} \frac{a_A^V}{a_A^S}]}, \quad (10)$$

that is also rewritten as

$$\frac{1}{a_a(A)} = \frac{1}{a_A^V} + \frac{A^{-1/3}}{a_A^S}. \quad (11)$$

As expected, the expressions [Eqs. (9)–(11)] are related to those from the earlier works [Eq. (2) and also see Eq. (21) in the next subsection, III B].

Here we would like to mention that Eqs. (10) and (2) are used in Ref. [55] as “definition I” [40,50,57] and “definition II” [58–60], respectively (see Eqs. (37) and (38) in Ref. [55]).

An important result that expresses the ratio of the volume to the surface energy coefficients by means of the shape of the symmetry energy dependence on density  $s(\rho)$  is given (in the local density approximation to the symmetry energy), e.g., in

Refs. [48,51] (see also Ref. [40]):

$$\frac{a_A^V}{a_A^S} = \frac{3}{r_0} \int dr \frac{\rho(r)}{\rho_0} \left\{ \frac{s(\rho_0)}{s[\rho(r)]} - 1 \right\}. \quad (12)$$

In Eq. (12)  $\rho(r)$  is the half-infinite nuclear matter density,  $\rho_0$  is the nuclear matter equilibrium density, and  $r_0$  is the radius of the nuclear volume per nucleon that can be obtained from

$$\frac{4\pi r_0^3}{3} = \frac{1}{\rho_0}. \quad (13)$$

For density-independent symmetry energy  $s(\rho) = s(\rho_0) = a_A^V$ , and then it follows from Eq. (12) that the ratio  $a_A^V/a_A^S = 0$  [48]. The density  $\rho(r)$  in Eq. (12) is uniform in two Cartesian directions and generally nonuniform in the third, usually chosen to be  $z$  [50]. The integral in Eq. (12) is across the nuclear surface involving the shape of the density dependence [41]. In Danielewicz's approximation only the symmetry energy of a finite nucleus  $a_a(A)$  has a mass dependence, while  $a_A^V$ ,  $a_A^S$ , and their ratio  $a_A^V/a_A^S$  are  $A$ -independent quantities. The values of  $a_A^V$  and  $a_A^S$  differ for various Skyrme interactions in wide intervals (see Table I of Ref. [50]). At the same time, as shown in [40], a combination of empirical data on skin sizes and masses of nuclei constrains the volume symmetry parameter to  $27 \leq a_A^V \leq 31$  MeV and the ratio  $a_A^V/a_A^S$  to  $2.0 \leq a_A^V/a_A^S \leq 2.8$ .

In the next section, III, we use the relationships from this section in order to consider the volume and surface components of the NSE and their ratio within the CDFM.

### III. THE CDFM. RESULTS OF CALCULATIONS OF NSE AND ITS VOLUME AND SURFACE CONTRIBUTIONS

#### A. The CDFM scheme to calculate the NSE

The CDFM was introduced and developed in Refs. [29,30] (and references therein). In the model the one-body density matrix  $\rho(\mathbf{r}, \mathbf{r}')$  of the nucleus is written as a coherent superposition of the one-body density matrices  $\rho_x(\mathbf{r}, \mathbf{r}')$  for spherical "pieces" of nuclear matter (so called "fluctons") with densities  $\rho_x(\mathbf{r}) = \rho_0(x)\Theta(x - |\mathbf{r}|)$ ,  $\rho_0(x) = 3A/4\pi x^3$ :

$$\rho(\mathbf{r}, \mathbf{r}') = \int_0^\infty dx |\mathcal{F}(x)|^2 \rho_x(\mathbf{r}, \mathbf{r}') \quad (14)$$

with

$$\rho_x(\mathbf{r}, \mathbf{r}') = 3\rho_0(x) \frac{j_1(k_F(x)|\mathbf{r} - \mathbf{r}'|)}{(k_F(x)|\mathbf{r} - \mathbf{r}'|)} \Theta\left(x - \frac{|\mathbf{r} + \mathbf{r}'|}{2}\right), \quad (15)$$

where  $j_1$  is the first-order spherical Bessel function and

$$k_F(x) = \left(\frac{3\pi^2}{2}\rho_0(x)\right)^{1/3} \equiv \frac{\beta}{x} \quad (16)$$

with

$$\beta = \left(\frac{9\pi A}{8}\right)^{1/3} \simeq 1.52A^{1/3} \quad (17)$$

is the Fermi momentum of the nucleons in the flucton with a radius  $x$ . It follows from Eqs. (14) and (15) that the density

distribution in the CDFM has the form

$$\rho(\mathbf{r}) = \int_0^\infty dx |\mathcal{F}(x)|^2 \rho_0(x) \Theta(x - |\mathbf{r}|). \quad (18)$$

The weight function  $|\mathcal{F}(x)|^2$  in Eq. (14) can be expressed using Eq. (18) by the density distribution  $\rho(r)$  and in the case of monotonically decreasing local density ( $d\rho/dr \leq 0$ ) can be obtained using a known density (from experiments or from theoretical models) for a given nucleus:

$$|\mathcal{F}(x)|^2 = -\frac{1}{\rho_0(x)} \left. \frac{d\rho(r)}{dr} \right|_{r=x} \quad (19)$$

with the normalization  $\int_0^\infty dx |\mathcal{F}(x)|^2 = 1$ .

The main assumption of the CDFM is that properties of finite nuclei can be calculated by expressions (obtained by using some approximations) that contain the corresponding quantities for nuclear matter folded with the weight function  $|\mathcal{F}(x)|^2$ . Then in the CDFM the symmetry energy  $s$  for finite nuclei is obtained to be an infinite superposition of the corresponding ANM symmetry energy weighted by  $|\mathcal{F}(x)|^2$ :

$$s = \int_0^\infty dx |\mathcal{F}(x)|^2 s^{\text{ANM}}(x). \quad (20)$$

The ANM quantity  $s^{\text{ANM}}(x)$  has to be determined within a chosen method for description of these characteristics. In our previous works [25,26,56] we have used for the matrix element  $V(x)$  of the nuclear Hamiltonian, as an example, the corresponding ANM energy from the energy density functional of Brueckner *et al.* [27,28]. The corresponding expression for  $s^{\text{ANM}}(x)$  within this method can be found in Refs. [25,26,56]. In these works we have calculated  $s$  using Eq. (20). In order to calculate the weight function  $|\mathcal{F}(x)|^2$  from Eq. (19) we used the calculated proton and neutron density distributions obtained from the self-consistent HF+BCS method from Ref. [33] (see also Ref. [61]) with density-dependent Skyrme interactions [32] and pairing correlations. In the method the pairing between like nucleons is included by solving the BCS equations at each iteration with a fixed pairing strength that reproduces the odd-even experimental mass differences [62]. The numerical results for  $s$  in spherical Ni, Sn, and Pb isotopic chains are given in Ref. [25], while for deformed exotic neutron-rich even-even Kr and Sm isotopes are presented in Ref. [26]. The density dependence of the NSE for neutron-rich and neutron-deficient Mg isotopes with  $A = 20-36$  is studied in Ref. [56].

In the end of this subsection we have to note, in order to avoid any misunderstanding, that the symmetry energy  $s$  (as well as the related quantities  $a_A^V$ ,  $a_A^S$ , and their ratio that are calculated in what follows in our work) are obtained within the CDFM using first the energy-density functional of Brueckner for the symmetry energy in infinite nuclear matter  $s^{\text{ANM}}$  in Eq. (20), while the weight function  $|\mathcal{F}(x)|^2$  is obtained using Eq. (19) by means of the density distribution calculated within the Skyrme HF+BCS method. Second, we calculate in the CDFM  $s$ ,  $a_A^V$ ,  $a_A^S$ , and  $a_A^V/a_A^S$  using as an additional example the Skyrme energy-density functional. In this case there is a self-consistency between the way to obtain  $|\mathcal{F}(x)|^2$  in the

Skyrme HF+BCS method and the use of the Skyrme EDF to obtain NSE and its components.

### B. Calculations of the volume and surface contributions to the NSE and their ratio within the CDFM

In the beginning of this subsection we show, first, that the expressions containing the coefficient  $a_a(A)$  [Eqs. (9) and (10)] (e.g., from [40,41,48,50,51]), as expected, can be represented approximately in the form of Eq. (2):

$$a_a(A) = \frac{a_A^V}{[1 + A^{-1/3} \frac{a_A^V}{a_A^S}]} \simeq c_3 - \frac{c_4}{A^{1/3}} \quad (21)$$

that corresponds to Eq. (7), if  $c_3 = a_A^V$  and  $c_4 = (a_A^V)^2/a_A^S$ . Equation (21) is obtained for large  $A$  (e.g., at least for  $A \geq 27$ ).

In the present paper we develop, using as a base Danielewicz's model [and specifically Eq. (12)], another approach to calculate the ratio  $a_A^V/a_A^S$ , as well as  $a_A^V$  and  $a_A^S$  within the CDFM. Our motivation is that numerous analyses of the volume and surface components of the NSE using a wide range of data on the binding energies, neutron-skin thicknesses, and excitation energies to IAS give estimations (presented later in our paper) of these quantities as functions of the mass number  $A$  (e.g., Refs. [16,38,39,49,51,63,64]) that change in some intervals for different regions of nuclei. For instance, the reported values of  $a_A^V$  and  $a_A^S$  are consistent with each other in a wide mass region ( $30 \leq A \leq 240$ ). In the CDFM we take nuclear matter values of the parameters to deduce their values in finite nuclei (using the self-consistently calculated nuclear density) which become dependent on the considered nucleus. For this purpose, we start from Eq. (12) but in it we replace the density  $\rho(r)$  for the half-infinite nuclear matter in the integrand by the density distribution of finite nucleus. Later, using Eq. (18) we obtain approximately an expression that allows us to calculate the ratio  $a_A^V/a_A^S$ . It has the form

$$\frac{a_A^V}{a_A^S} = \frac{3}{r_0 \rho_0} \int_0^\infty dx |\mathcal{F}(x)|^2 x \rho_0(x) \left\{ \frac{s(\rho_0)}{s[\rho_0(x)]} - 1 \right\}. \quad (22)$$

The approximations made in the CDFM lead to one-dimensional integral over  $x$ , the latter being the radius of the "flucton" that is perpendicular to the nuclear surface. Here we would like to emphasize that, in contrast to Eq. (12), in Eq. (22) we use the finite nuclei densities to calculate the weight function  $|\mathcal{F}(x)|^2$ . In this way, the integral in Eq. (22) contains shell effects (different from the Friedel oscillations [65,66] present in any quantal calculations of semi-infinite nuclear matter) and curvature contributions. Thus, caution is necessary when considering the role of these effects on the key quantity  $a_A^V/a_A^S$  ratio. The procedure to go from infinite  $A$  to finite  $A$  that we follow to go from Eq. (12) to Eq. (22) is the same that we have followed for other nuclear properties within the CDFM, so there is no conceptual inconsistency.

The purpose of our approach is to use the CDFM not only to calculate the NSE  $s$ , but also the ratio  $a_A^V/a_A^S$  and  $a_A^V$  and  $a_A^S$  separately. Thus, the calculation of these quantities in the same model leads to a self-consistency. As will be shown later in the paper, in the CDFM the dependence of  $a_A^V$  and  $a_A^S$  on  $A$

turns out to be weak. The differences within a given isotopic chain are approximately between 0.5 and 1.5 MeV. They are narrower than the differences in Danielewicz's approach using in the calculations different Skyrme forces (e.g., Table I of Ref. [50]). We note that our method is different from that of Danielewicz. Starting from Eq. (12), the approximation of the CDFM enables us to use not the half-infinite nuclear matter density but densities of finite nuclei. The results turn out to be consistent with the large amount of empirical data, as will be shown below. The spirit of our approach is in some sense opposite to what it was done in the past. For instance, in the LDM mass formula one takes empirical mass values of finite nuclei to extract "A-independent" values of the parameters, some of which are afterwards extrapolated to nuclear matter energy density functionals, e.g., in the Brueckner EDF. The Danielewicz's formalism is on these lines, but parametrizes surface effects through half-infinite nuclear matter. In Eq. (22)  $s(\rho_0) = s^{\text{ANM}}(\rho_0)$  and the quantity  $s[\rho_0(x)] = s^{\text{ANM}}[\rho_0(x)]$  is the NSE within the chosen approach for the EDF. From Eqs. (19) and (20) we obtain the CDFM value for the NSE,

$$s \equiv a_a(A). \quad (23)$$

Let denote by

$$\kappa \equiv \frac{a_A^V}{a_A^S} \quad (24)$$

that can be calculated using Eq. (22). Then it follows from Eq. (10)

$$s = \frac{a_A^V}{1 + A^{-1/3} \kappa}. \quad (25)$$

Finally, as a next step we obtain from Eqs. (23)–(25) (having calculated within the CDFM the values of  $s$  and  $\kappa$ ) the expressions from which we can estimate the values of  $a_A^V$  and  $a_A^S$  separately:

$$a_A^V = s(1 + A^{-1/3} \kappa), \quad (26)$$

$$a_A^S = \frac{s}{\kappa}(1 + A^{-1/3} \kappa). \quad (27)$$

In our work we use two energy-density functionals. The first one is the Brueckner EDF [27,28]. It was used in our previous works [25,26,56] to calculate the NSE  $s$  using Eq. (20). In this approach the value of the equilibrium nuclear matter density is  $\rho_0 = 0.204 \text{ fm}^{-3}$ ,  $r_0 = 1.054 \text{ fm}$  [obtained from Eq. (13)], and the symmetry energy at equilibrium nuclear matter density  $s(\rho_0)$  in Eq. (22) is equal to 35.07 MeV. In the case of the Brueckner EDF the results of the calculations using Eq. (22) of the ratio  $\kappa$  as a function of the mass number  $A$  for the isotopic chains of Ni, Sn, and Pb with different forces (SLy4, SGII, and Sk3) are given in Figs. 1–3, respectively. By means of Eqs. (26) and (27) and the values of the NSE obtained in our works [25,26], we calculated the coefficients  $a_A^V$  and  $a_A^S$ . Their values as functions of  $A$  for the same isotopic chains are presented in Figs. 4–6, respectively.

It can be seen from Figs. 1–3 that our results for the values of the ratio  $\kappa$  are within the range

$$2.10 \leq \kappa \leq 2.90. \quad (28)$$

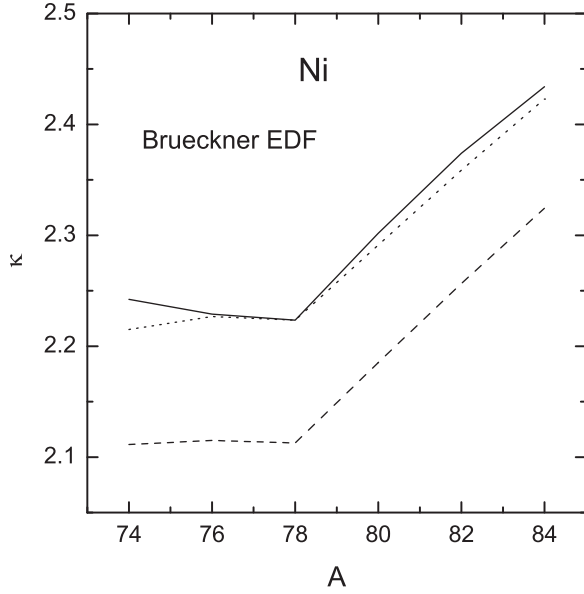


FIG. 1. The ratio  $\kappa = a_A^V/a_A^S$  as a function of  $A$  for the isotopic chain of Ni. The SLy4 (solid line), SGII (dashed line), and Sk3 (dotted line) forces have been used in the HF+BCS calculations of the densities in the case of Brueckner EDF.

This range of values is similar to the estimations of Danielewicz *et al.* obtained from a wide range of available data on the binding energies and from fits to other nuclear properties, such as the neutron-skin thickness and the excitation energies to the IAS [41] (for definitions and examples of IAS, see, e.g., Ref. [45]). As already mentioned, it has been shown in Ref. [40] that a combination of masses and neutron-skin sizes constrains the values of the volume symmetry parameter between 27 and 31 MeV and the value of the volume to surface-symmetry parameter ratio between 2.0 and 2.8. The minimum value of the ratio obtained in Ref. [40] is 1.7. The

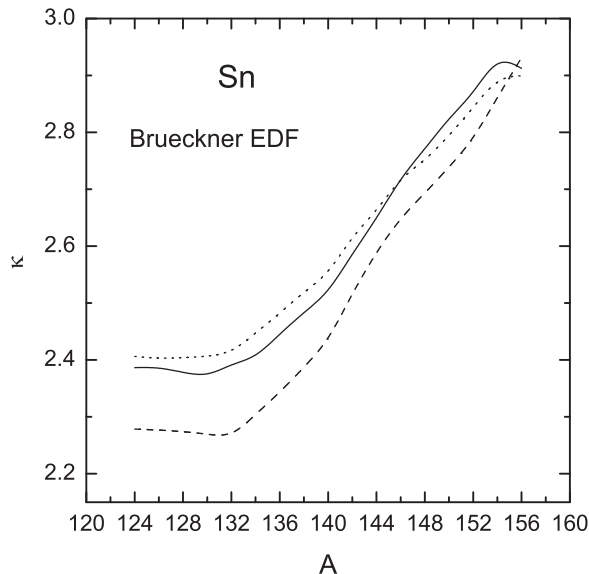


FIG. 2. The same as in Fig. 1 but for the isotopic chain of Sn.

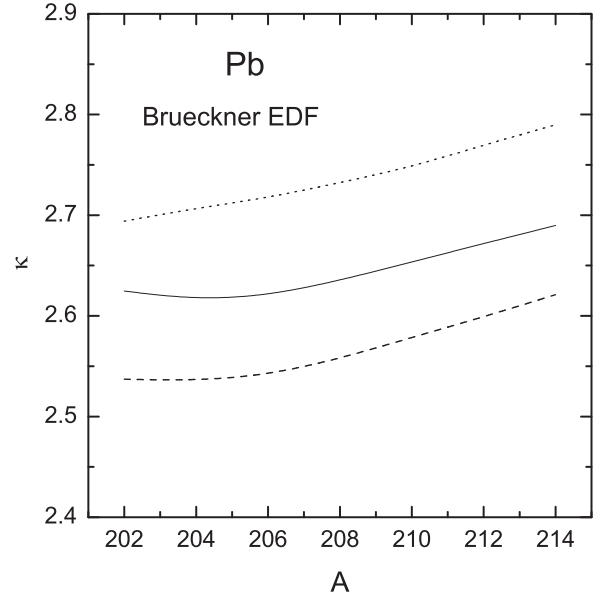


FIG. 3. The same as in Fig. 1 but for the isotopic chain of Pb.

ranges of the published values of the ratio  $\kappa$  extracted from nuclear properties and presented in Ref. [51] are (see Table II in [51]):

$$2.6 \leq \kappa \leq 3.0 \quad (29)$$

from IAS and skins [41],

$$2.0 \leq \kappa \leq 2.8 \quad (30)$$

from masses and skins [40], and

$$1.6 \leq \kappa \leq 2.0 \quad (31)$$

from the analyses in Ref. [51] of masses and skins. As can be seen, the ranges (29) and (30) are in a good agreement with our results [see Eq. (28)].

As can be seen in Fig. 1, there exists a “kink” in the curve of  $\kappa \equiv a_A^V/a_A^S$  as a function of  $A$  for the double-magic  $^{78}\text{Ni}$  nucleus. Such a kink exists also for the double-magic  $^{132}\text{Sn}$  nucleus that can be seen in Fig. 2. Here we would like to note that the origin of the kinks is in the different behaviors of the density distributions  $\rho(r)$  for given isotopes. Namely the derivative of  $\rho(r)$  determines the weight function  $|\mathcal{F}(x)|^2$  [Eq. (19)] that takes part in the integrand of the integral in Eq. (22) giving the ratio  $\kappa \equiv a_A^V/a_A^S$ . The peculiarities of  $\rho(r)$  for the closed shells lead to the existence of kinks. As shown in more details in Ref. [26], this is the reason for the kinks in the NSE  $s(A)$ , as can be seen in the expression for it [see Eq. (20)]. The kink of  $s(A)$  at  $^{78}\text{Ni}$  can be seen in Fig. 2 of Ref. [25], and the kink of  $s(A)$  for  $^{132}\text{Sn}$  in Fig. 8 of the same paper. In the case of Pb isotopic chain (see Fig. 3) such kinks do not exist and this reflects the smooth behavior without kinks of  $s(A)$  and related quantities for the Pb isotopic chain [25,26].

It is seen from Figs. 4–6 that our CDMF results obtained with Brueckner EDF for  $a_A^V$  are between 41.5 and 43 MeV, while for  $a_A^S$  they are between 14 and 20 MeV. These values are somewhat larger than those from other references given above. As can be seen from Eqs. (26) and (27), these differences are

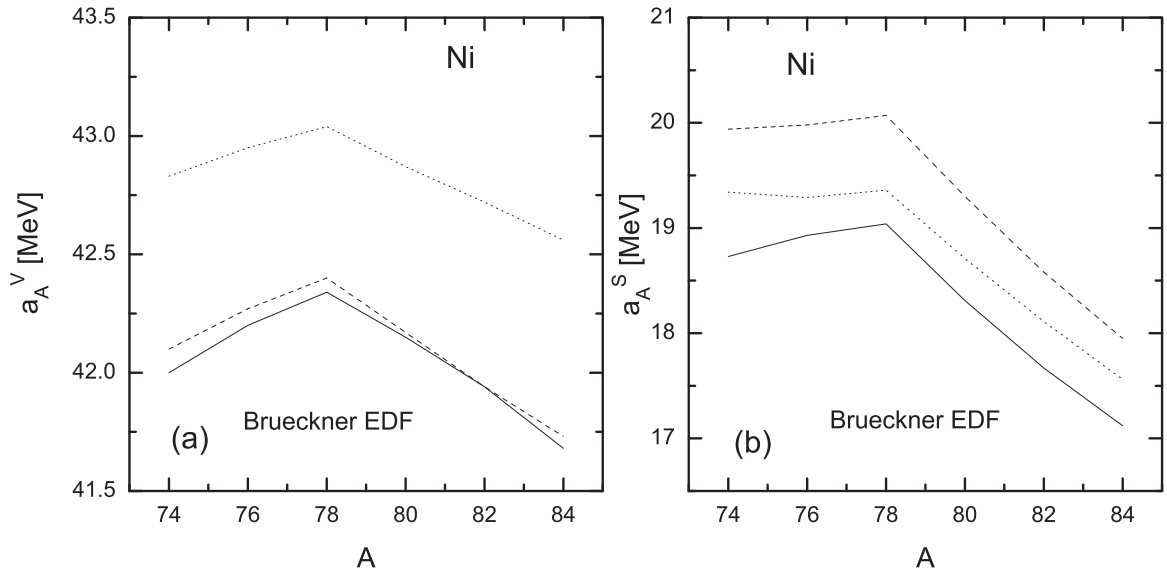


FIG. 4. The values of  $a_A^V$  (a) and  $a_A^S$  (b) as functions of  $A$  for the isotopic chain of Ni. The SLy4 (solid line), SGII (dashed line), and Sk3 (dotted line) forces have been used in the HF+BCS calculations of the densities in the case of Brueckner EDF.

due mainly to the somewhat larger values of the NSE ( $s$ ) for finite nuclei obtained within the CDFM using the Brueckner functional, because our values for the component  $\kappa = a_A^V/a_A^S$  (that are between 2.1 and 2.9) are in the range obtained by other authors. The ranges of changes of our results for  $a_A^V$  and  $a_A^S$  in the case of the Brueckner EDF depend on the Skyrme forces used in the HF+BCS calculations of the nuclear densities. They are given in Table I together with their corresponding average values for each force and isotopic chain. These results can be compared with the results obtained in

- Ref. [40]:  $27 \leq \alpha = a_A^V \leq 31$  MeV;
- Ref. [41]:  $30.0 \leq a_A^V \leq 32.5$  MeV;
- Ref. [50]:  $31.5 \leq a_A^V \leq 33.5$  MeV,  $9 \leq a_A^S \leq 12$  MeV;
- Ref. [42]:  $30.2 \leq a_A^V \leq 33.7$  MeV.

It is shown in Ref. [42] that at  $A \geq 30$   $a_A^V \approx 33.2$  MeV and  $a_A^S \approx 10.7$  MeV.

For completeness and better comparison we list below also the results presented in Ref. [42], making reference to Ref. [16]  $a_A^V = 39.73$  MeV and  $a_A^S = 8.48$  MeV, to Ref. [63]  $a_A^V = 31.74$  MeV and  $a_A^S = 11.27$  MeV, and to Ref. [64]  $a_A^V = 35.51$  MeV and  $a_A^S = 9.89$  MeV. These results are consistent with each other in the region  $30 \leq A \leq 240$ . In the latter mass region the averaged values obtained are (i)  $a_A^V \approx 35.34$  MeV and  $a_A^S \approx 9.67$  MeV in Ref. [42]; (ii)  $30 \leq a_A^V \leq 32.5$  MeV in Ref. [48]; and (iii)  $30 \leq a_A^V \leq 33$  MeV and  $a_A^S \approx 11.3$  MeV in Ref. [43].

We would like to note that the same peculiarities (as for the ratio  $\kappa \equiv a_A^V/a_A^S$ ), namely “kinks,” appear in the cases of  $a_A^V$  and  $a_A^S$  as functions of the mass number  $A$ . In Figs. 4(a)

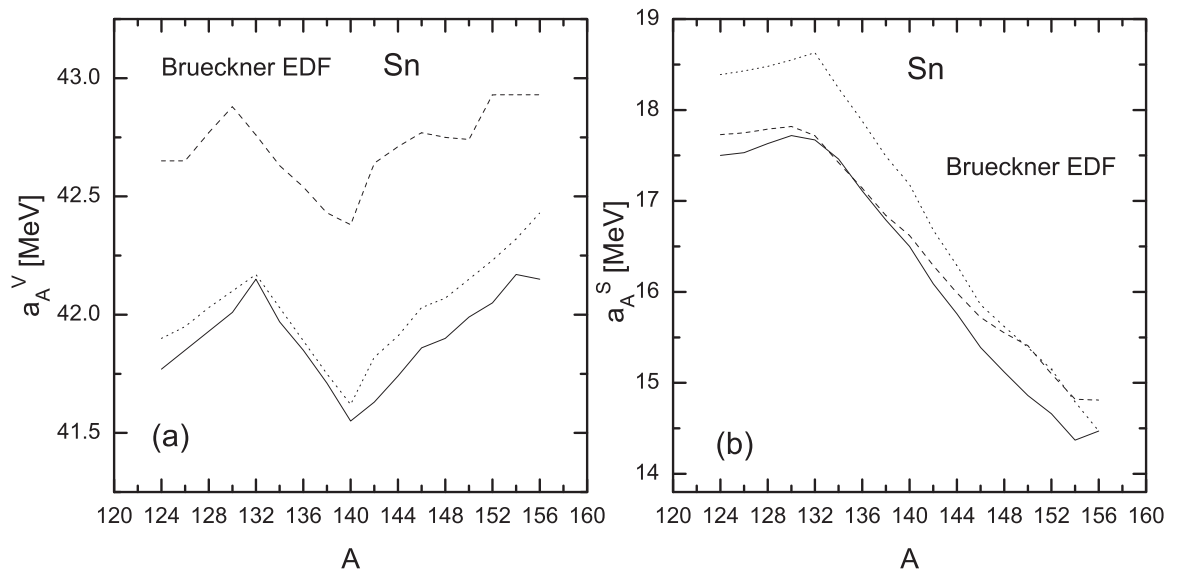


FIG. 5. The same as in Fig. 4 but for the isotopic chain of Sn.

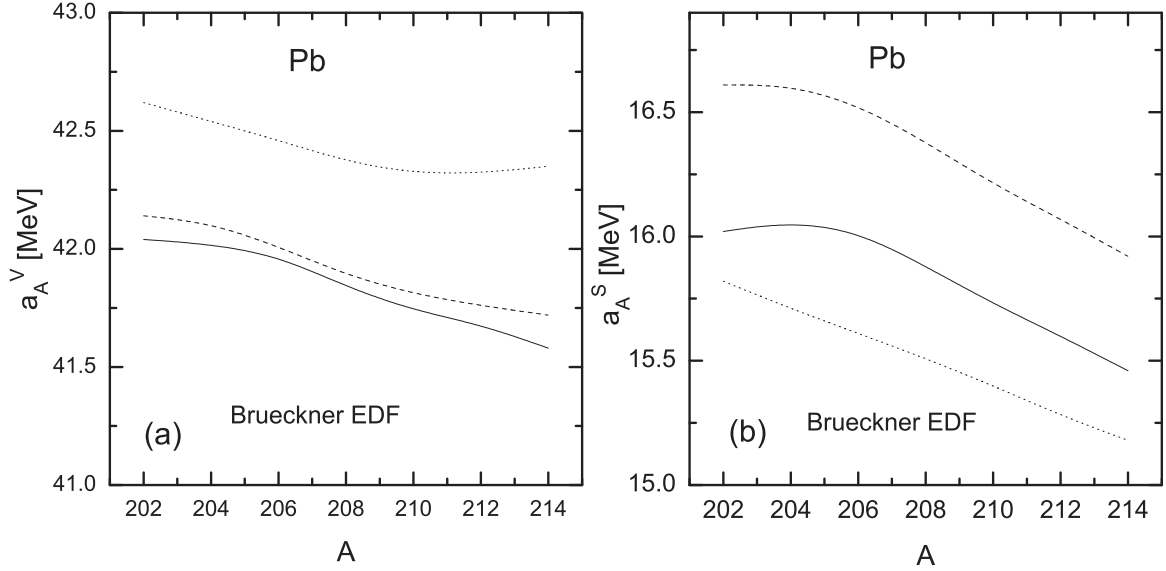


FIG. 6. The same as in Fig. 4 but for the isotopic chain of Pb.

and 4(b) one can see kinks for  $a_A^V$  and  $a_A^S$ , respectively, in the case of the double-magic nucleus  $^{78}\text{Ni}$ . In Fig. 5(a) a kink appears for  $a_A^V(A)$  not only for the double-magic  $^{132}\text{Sn}$  but also for the semimagic  $^{140}\text{Sn}$  nucleus. The latter is related to the closed  $2f_{7/2}$  subshell for neutrons. The behavior of  $a_A^S(A)$  does not allow a corresponding “kink” for  $^{140}\text{Sn}$  to be visible in the ratio  $\kappa \equiv a_A^V/a_A^S$ . Reiss *et al.* discussed in Ref. [67] that the region around  $N = 90$  for neutron-rich tin isotopes is an interesting one because the shell structure is somewhat fluctuating. Although the average gap at  $N = 90$  was found to be small, there are indications of a weak subshell closure, the latter being supported also by the small jump in the two-neutron separation energy in the same region, both calculated at zero temperature [67]. In addition, in Ref. [68]  $N = 90$

was predicted to be submagic with Gogny D1S and D1M interactions at  $^{140}\text{Sn}$  because the  $2f_{7/2}$  orbit is fully occupied, but not with M3Y-P6 and P7 semirealistic NN interactions. As can be seen from Eqs. (26) and (27), the reason for kinks in the separate coefficients as functions of  $A$  is twofold. One of them is the already mentioned reason for the kinks in the ratio  $\kappa \equiv a_A^V/a_A^S$ , while the same reason causes also kinks in the NSE ( $s$ ) at closed-shell nuclei.

The second EDF that we use in the calculations is that one of Skyrme with different Skyrme forces (e.g., Ref. [69]). The aim to use this EDF is twofold: (i) we can compare the values of our  $A$ -dependent quantities  $a_A^V$ ,  $a_A^S$ , and  $\kappa \equiv a_A^V/a_A^S$  obtained in the CDFM with the  $A$ -independent ones obtained in Danielewicz’s approximation (e.g., [40,50]), and (ii) the nuclear densities are obtained using the same Skyrme forces as in the HF+BCS calculations, so there is a self-consistency

TABLE I. The ranges of changes of  $a_A^V$  and  $a_A^S$  and their average values for SLy4, SGII, and Sk3 forces used in the HF+BCS calculations of the nuclear densities with Brueckner EDF for the Ni, Sn, and Pb isotopic chains.

Isotopic chain	NSE component	SLy4	SGII	Sk3
Ni	$a_A^V$	41.7–42.3	41.7–42.4	42.6–43
	$a_A^S$	17.1–19	18–20	17.6–19.4
	$\bar{a}_A^V$	42.05	42.1	42.83
	$\bar{a}_A^S$	18.3	19	18.73
Sn	$a_A^V$	41.6–42.2	42.4–43	41.6–42.4
	$a_A^S$	14.4–17.7	14.8–17.8	14.5–18.6
	$\bar{a}_A^V$	41.9	42.71	42.02
	$\bar{a}_A^S$	16.27	16.5	16.92
Pb	$a_A^V$	41.6–42	41.7–42.1	42.3–42.6
	$a_A^S$	15.5–16.1	16–16.6	15.2–15.8
	$\bar{a}_A^V$	41.84	41.92	42.43
	$\bar{a}_A^S$	15.82	16.33	15.5

TABLE II. The parameters of SGII, Sk3, and SLy4 Skyrme forces in the Skyrme EDF, the spin-orbit parameter  $W_0$ , the ANM equilibrium density  $\rho_0$ ,  $r_0$ , and the symmetry energy at equilibrium density  $s(\rho_0)$ .

	SGII	Sk3	SLy4
$t_0$ (MeV fm <sup>3</sup> )	−2645.0	−1128.75	−2488.91
$t_1$ (MeV fm <sup>5</sup> )	340.0	395.0	486.82
$t_2$ (MeV fm <sup>5</sup> )	−41.9	−95.0	−546.39
$t_3$ (MeV fm <sup>3+3σ</sup> )	15595.0	14000.0	13777.0
$x_0$	0.09	0.45	0.834
$x_1$	−0.0588	0	−0.344
$x_2$	1.425	0	−1.0
$x_3$	0.06044	1.0	1.354
$\sigma$	0.16667	1.0	0.16667
$W_0$	105.0	120.0	123.0
$\rho_0$ (fm <sup>−3</sup> )	0.1583	0.1453	0.1595
$r_0$ (fm)	1.147	1.18	1.144
$s(\rho_0)$ (MeV)	26.84	28.17	32.01

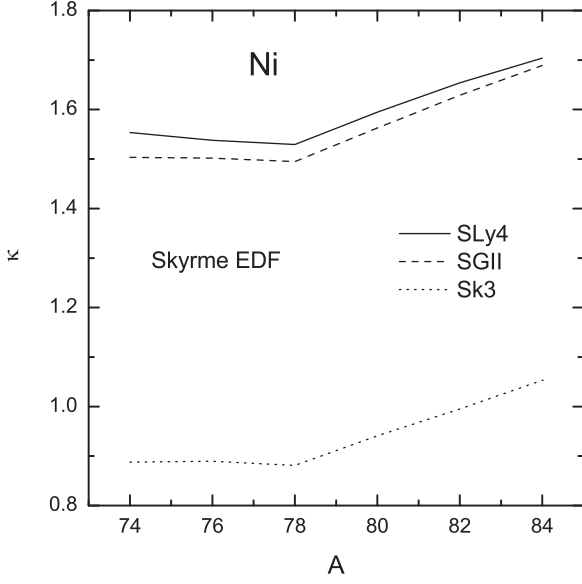


FIG. 7. The ratio  $\kappa = a_A^V/a_A^S$  as a function of  $A$  for the isotopic chain of Ni in the case of Skyrme EDF with use of SLy4, SGII, and Sk3 forces.

of the approach. In the standard Skyrme EDF the symmetry energy  $s_{Sk}[\rho_0(x)]$  of nuclear matter with density  $\rho_0(x)$  can be expressed by (e.g., Ref. [70])

$$s_{Sk}[\rho_0(x)] = \frac{\hbar^2}{6m} \left( \frac{3\pi^2}{2} \right)^{2/3} \rho_0^{2/3}(x) - \frac{1}{8} t_0 (1 + 2x_0) \rho_0(x) - \frac{1}{48} t_3 (1 + 2x_3) \rho_0^{\sigma+1}(x) - \frac{1}{24} \left( \frac{3\pi^2}{2} \right)^{2/3} \times [3t_1 x_1 - t_2 (4 + 5x_2)] \rho_0^{5/3}(x). \quad (32)$$

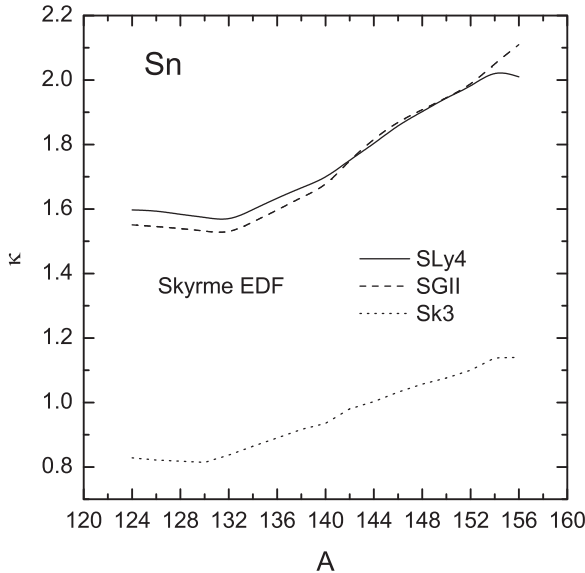


FIG. 8. The same as in Fig. 7 but for the isotopic chain of Sn.

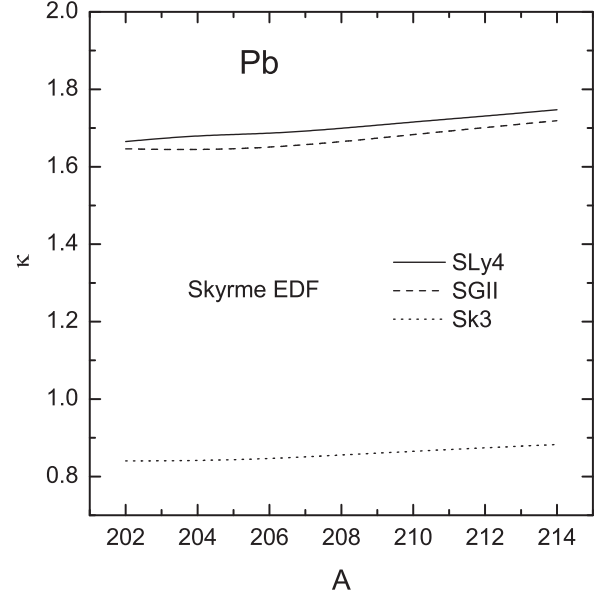


FIG. 9. The same as in Fig. 7 but for the isotopic chain of Pb.

The parameters of SGII, Sk3, and SLy4 Skyrme forces used to calculate the symmetry energy of ANM, as well as the values of the nuclear matter equilibrium density  $\rho_0$ ,  $r_0$ , and the symmetry energy at equilibrium density  $s(\rho_0)$ , are listed in Table II. In addition, in the same Table we give the values of the spin-orbit parameter  $W_0$  used in the HF+BCS calculations of the density distributions for the three Skyrme forces.

The values of  $\kappa$  for the three isotopic chains (of Ni, Sn, and Pb) obtained using SLy4, SGII, and Sk3 forces are given in Figs. 7–9 and those of  $a_A^V$  and  $a_A^S$  are presented in Figs. 10–12. The ranges of changes of the latter, as well as their average values, are given in Table III.

As can be seen from Figs. 7–9 the ranges of changes of  $\kappa$  are, for the Ni isotopic chain,  $1.5 \leq \kappa \leq 1.7$  (SLy4 and SGII forces) and  $0.88 \leq \kappa \leq 1.05$  (Sk3 force); for the Sn isotopic chain,  $1.52 \leq \kappa \leq 2.1$  (SLy4 and SGII forces) and  $0.82 \leq \kappa \leq 1.14$  (Sk3 force); and for the Pb isotopic chain,  $1.65 \leq \kappa \leq 1.75$  (SLy4 and SGII forces) and  $0.84 \leq \kappa \leq 0.88$  (Sk3 force). We note that the ranges of  $\kappa$  for the SLy4 and SGII forces in the three chains are in agreement with those obtained in Ref. [51]  $1.6 \leq \kappa \leq 2.0$  from analyses of masses and skins.

What can be seen in Figs. 10–12 is that the values of  $a_A^V$  are almost independent of  $A$  for a given isotopic chain and Skyrme force. They are also similar in the different chains for a given Skyrme force. The comparison of the results of our approach with those of other authors shows that our values of  $a_A^V$  for the isotopic chains of Ni, Sn, and Pb for the SGII and Sk3 forces are in agreement with those from, e.g., Refs. [40,42,43,48,50] given above, while the obtained values for the SLy4 force are comparable with the results in Ref. [16]. One can see also a kink in the behavior of  $\kappa$  for the Ni chain at  $A = 78$ , for the Sn chain at  $A = 132$ , and a lack of kinks for the Pb chain, like in the case when the Brueckner EDF is used. A kink for the Ni chain at  $A = 78$  can be seen also in the  $A$  dependence of  $a_A^S$ ; as well, a kink of  $a_A^S$  is seen at  $A = 132$  in the case of the Sn chain. In the latter, small kinks can be observed also for  $a_A^V$

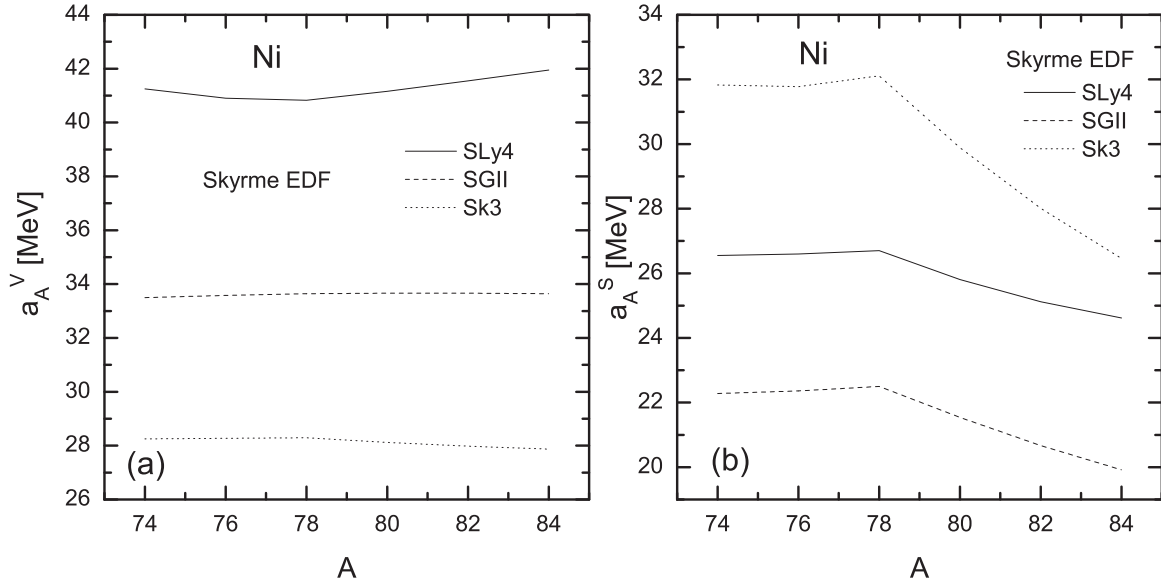


FIG. 10. The values of  $a_A^V$  (a) and  $a_A^S$  (b) as functions of  $A$  for the isotopic chain of Ni in the case of Skyrme EDF with use of SLy4, SGII, and Sk3 forces.

especially at  $A = 132$  for the SLy4 force. There are no kinks of  $a_A^V$  and  $a_A^S$  in the Pb chain.

In the end of this section we would like to note that the obtained values of  $\kappa \equiv a_A^V/a_A^S$  in the CDFM [Eq. (28)], that are in agreement with the recently published values [Eq. (29)], are quite different from the value of  $\chi \equiv c_4/c_3$  from Eq. (3) estimated to be 1.1838 [15] or 1.14 [36]. [We mention that according to Eq. (21) (and the text after it), for large  $A$ ,  $c_4/c_3 \simeq a_A^V/a_A^S$ . This difference will be reflected in the corresponding values of  $c_3$  and  $c_4$  that can be obtained using Eq. (8).

#### IV. CONCLUSIONS

In the present work we study the volume and surface components of the NSE as well as their ratio within the framework of the CDFM. This consideration is based on the calculations of the total NSE that have been performed in our previous works [25,26,56], and also uses the results of the earlier works on the subject (see, e.g., [15,34–37]), as well as the later theoretical approaches of Warda *et al.* [38], Centelles *et al.* [39], Danielewicz *et al.* (e.g., [40–48,50], Dieperink and Van Isacker [51], and others.

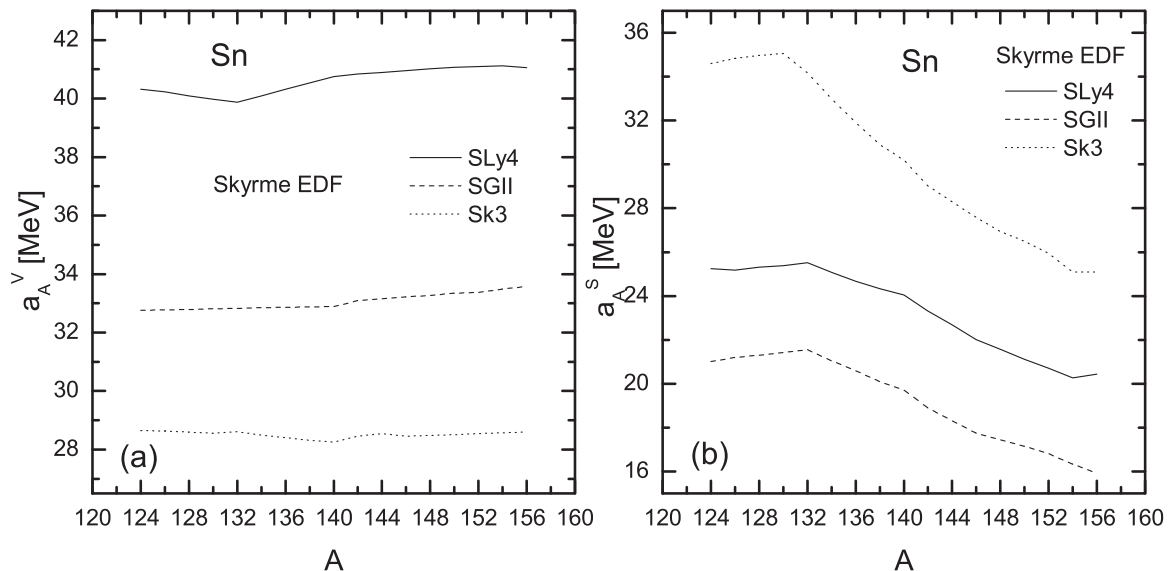


FIG. 11. The same as in Fig. 10 but for the isotopic chain of Sn.

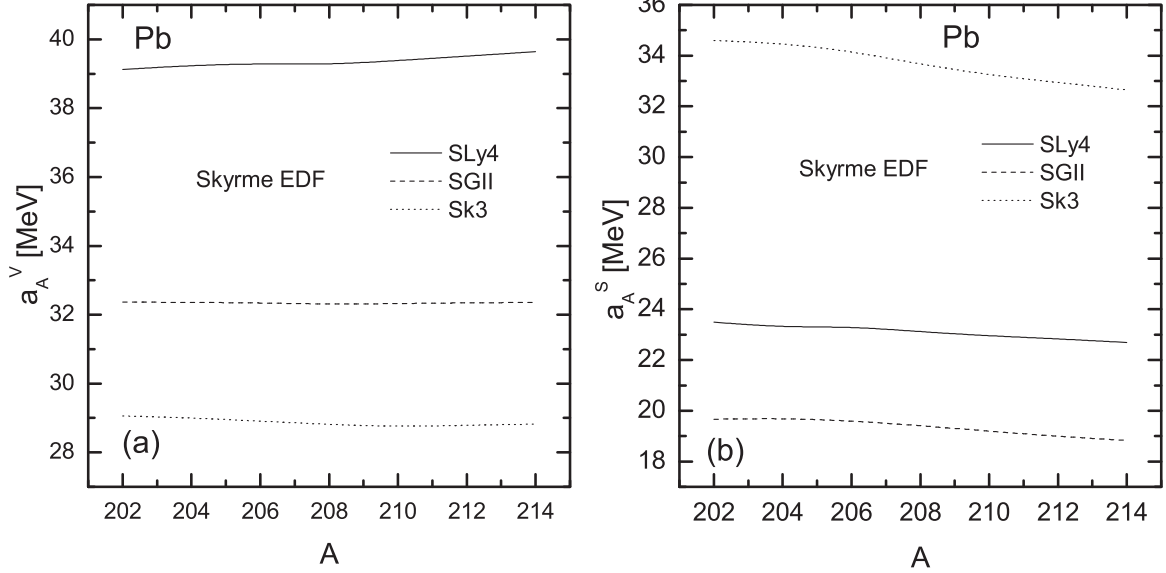


FIG. 12. The same as in Fig. 10 but for the isotopic chain of Pb.

The results can be summarized as follows:

- (i) We develop, using as a base Danielewicz's model [Eq. (12)], another approach within the CDFM to calculate the ratio  $a_A^V/a_A^S$  between the volume and surface components of the symmetry energy  $s$ , as well as  $a_A^V$  and  $a_A^S$  separately, for finite nuclei. We obtain within the CDFM the expression for  $\kappa \equiv a_A^V/a_A^S$  [Eq. (22)] that allows us to calculate this ratio using the ingredients of the model, the weight function  $|\mathcal{F}(x)|^2$  and the nuclear matter symmetry energy  $s^{\text{ANM}}[\rho_0(x)]$  from two energy-density functionals, the Brueckner and Skyrme ones. The first one of them was used to calculate the NSE in our previous works [25,26,56]. In the CDFM we take nuclear matter values of the components of NSE to deduce their values in finite nuclei.

TABLE III. The ranges of changes of  $a_A^V$  and  $a_A^S$  and their average values for SLy4, SGII, and Sk3 forces used in the calculations with Skyrme EDF for the Ni, Sn, and Pb isotopic chains.

Isotopic chain	NSE component	SLy4	SGII	Sk3
Ni	$a_A^V$	40.8–42	33.5–33.7	27.9–28.3
	$a_A^S$	24.6–26.7	20–22.5	26.5–32.1
	$\bar{a}_A^V$	41.27	33.61	28.13
	$\bar{a}_A^S$	25.9	21.55	30.01
Sn	$a_A^V$	40–41.1	32.8–33.6	28.3–28.6
	$a_A^S$	20.3–25.5	16–21.5	25.1–35
	$\bar{a}_A^V$	40.6	33.06	28.51
	$\bar{a}_A^S$	23.36	19.21	30.24
Pb	$a_A^V$	39.1–39.6	32.3–32.4	28.8–29.1
	$a_A^S$	22.7–23.5	18.8–19.7	32.7–34.6
	$\bar{a}_A^V$	39.35	32.34	28.88
	$\bar{a}_A^S$	23.1	19.34	33.68

Thus, our approach is different from the Danielewicz's formalism. Being motivated by the available empirical data that show  $A$  dependence of  $a_A^V$ ,  $a_A^S$ , and their ratio, we obtained in our approach a possibility to find a (weak)  $A$  dependence of the theoretical results for these quantities within the CDFM. The weight function  $|\mathcal{F}(x)|^2$  [Eq. (19)] is calculated using the proton and neutron density distributions obtained from the self-consistent deformed HF+BCS method [33,61] with density-dependent Skyrme interactions.

- (ii) The values of  $\kappa$  calculated using the Brueckner EDF for the isotopic chains of Ni, Sn, and Pb are between 2.10 and 2.90. This range of values is similar to the estimations of Danielewicz *et al.* obtained from a wide range of available data on the binding energies [40], of Steiner *et al.* [49], and from a fit to other nuclear properties, such as the excitation energies to IAS [41], neutron-skin thickness, and others. The values of  $\kappa$  obtained using the Skyrme EDF for the same isotopic chains with SLy4, SGII, and Sk3 forces are between 1.5 and 2.1 for the SLy4 and SGII forces and between 0.82 and 1.14 for the Sk3 force. The former result is in agreement with that obtained in Ref. [51]:  $1.6 \leq \kappa \leq 2.0$  from the analyses of masses and skins.
- (iii) We calculate the values of the volume and surface contributions to the NSE by means of Eqs. (26) and (27) within the CDFM. The values of NSE are taken from our previous works [25,26,56], where we used first the Brueckner EDF. The range of the values obtained for the volume symmetry energy coefficient  $a_A^V$  (between 41.5 and 43 MeV) is narrower than the one of the surface symmetry energy coefficient  $a_A^S$  (between 14 and 20 MeV). The values of both coefficients are somewhat larger than the already mentioned values of other works (see, e.g., [16,40–43,48,63,64] and others). We relate this difference to the larger values of the total NSE for finite nuclei

calculated by the use of the Brueckner approach [27,28] within the CDFM [25,26,56]. Second, the  $a_A^V$  and  $a_A^S$  are calculated within our approach using the Skyrme EDF. It can be seen that the values of  $a_A^V$  are almost constant as functions of  $A$  for a given isotopic chain and Skyrme force. They are also similar in the considered chains for a given Skyrme force. Our values of  $a_A^V$  for the isotopic chains of Ni, Sn, and Pb for the SGII and Sk3 forces are in agreement with those from, e.g., Refs. [40,42,43,48,50], while those in the case of the SLy4 force are similar to the results presented in Refs. [16,42]. We note that instead of the Brueckner and Skyrme EDFs that are used in the present work as examples, one can apply also other realistic functionals, like the recently proposed Kohn-Sham EDF based on microscopic nuclear and neutron matter equations of state [71].

- (iv) Studying first the isotopic sensitivity of  $a_A^V$ ,  $a_A^S$ , and their ratio in the case of using the Brueckner EDF we observe peculiarities (“kinks”) of these quantities as functions of the mass number  $A$  in the cases of the double-magic  $^{78}\text{Ni}$  and  $^{132}\text{Sn}$  isotopes for  $\kappa \equiv a_A^V/a_A^S$ ,  $a_A^V$ , and  $a_A^S$ , as well as a “kink” of  $a_A^V$  for  $^{140}\text{Sn}$ . The latter is related to the closed  $2f_{7/2}$  subshell for neutrons. The origin of the kinks is in the different behaviors of the density distributions  $\rho(r)$  for the isotopes, because the derivative of  $\rho(r)$  determines the weight function  $|\mathcal{F}(x)|^2$  [Eq. (19)] that takes part in the expression for the ratio  $\kappa \equiv a_A^V/a_A^S$  [Eq. (22)]. As shown in Ref. [26], this is the reason for the kinks in the NSE ( $s$ ) [see Eq. (20)] observed in our previous works [25,26]. Similarly to the case when Brueckner EDF is used, in the case of the Skyrme EDF one can see also a kink in the behavior of  $\kappa$  for the chain of Ni at  $A = 78$  (Fig. 7) and for the Sn chain at  $A = 132$  (Fig. 8), as well as a lack of kinks for the Pb case (Fig. 9). A kink in the Ni chain at  $A = 78$  can be seen also in the  $A$  dependence of  $a_A^S$  [Fig. 10(b)], as well as of  $a_A^S$  at  $A = 132$  in the case of the Sn chain [Fig. 11(b)]. In Fig. 11(a) small kinks can be observed also for  $a_A^V$  especially at  $A = 132$  for the SLy4 and Sk3 forces. Kinks of the  $A$  dependence of  $a_A^V$  and  $a_A^S$  in the Pb isotopic chain are not observed.

- (v) We show in Sec. III B that, as expected, the expression for the coefficient of the symmetry energy  $a_a(A)$  [Eq. (10)] used, e.g., in Refs. [40,41,48,50,51], can be approximately written for large  $A$  in the form of Eqs. (2), (7), and (21) introduced by Cameron [35] and used by Bethe [36], Myers and Swiatecki [15], and others. We note that the obtained values of  $\kappa \equiv a_A^V/a_A^S$  in the CDFM using Brueckner and Skyrme EDFs that are in agreement with the recently published values are quite different from the value  $\chi \equiv c_4/c_3$  [Eq. (3)] that is estimated to be 1.1838 [15] or 1.14 [36] [having in mind that, for large  $A$ ,  $c_4/c_3 \simeq a_A^V/a_A^S \equiv \kappa$ ; see Eq. (21)].

The suggested approach using the CDFM and based on a given EDF and self-consistent mean-field method makes it possible to start with the global values of parameters for infinite nuclear matter and to derive their corresponding values in finite nuclei, which become  $A$  dependent. This is the main difference from other approaches. The method uses the symmetry energy coefficient  $s = a_a(A)$  obtained within the CDFM in finite nuclei [25,26,56] in the case of the Brueckner EDF, as well as the NSE calculated in the present work in the case of the Skyrme EDF. The calculation of the latter avoids the problem related to fitting the Hartree-Fock energies to LDM parametrization. The method makes it possible to obtain in the present work additional information not only about the volume contribution  $a_A^V$  to the symmetry energy, but also about the surface symmetry energy term  $a_A^S$  of the LDM, as well as to establish their eventual  $A$ -dependence. As known, the  $a_A^S$  is poorly constrained by empirical data. The obtained results could provide a possibility to test the properties of the nuclear energy density functionals and characteristics related to NSE, e.g., the neutron skin thickness of finite nuclei.

#### ACKNOWLEDGMENTS

Two of the authors (A.N.A. and M.K.G.) are grateful for support of the Bulgarian Science Fund under Contract No. DFNI-T02/19. E.M.G. and P.S. acknowledge support from MINECO (Spain) under Contract FIS2014-51971-P.

- [1] M. Centelles, X. Roca-Maza, X. Viñas, and M. Warda, *Phys. Rev. Lett.* **102**, 122502 (2009).  
 [2] P. Danielewicz, R. Lacey, and W. G. Lynch, *Science* **298**, 1592 (2002).  
 [3] D. V. Shetty, S. J. Yennello, and G. A. Souliotis, *Phys. Rev. C* **76**, 024606 (2007).  
 [4] M. A. Famiano, T. Liu, W. G. Lynch, M. Mocko, A. M. Rogers, M. B. Tsang, M. S. Wallace, R. J. Charity, S. Komarov, D. G. Sarantites, L. G. Sobotka, and G. Verde, *Phys. Rev. Lett.* **97**, 052701 (2006).  
 [5] D. V. Shetty and S. J. Yennello, *Pramana* **75**, 259 (2010).  
 [6] A. Klimkiewicz, N. Paar, P. Adrich, M. Fallot, K. Boretzky, T. Aumann, D. Cortina-Gil, U. DattaPramanik, T. W. Elze, H. Emling, H. Geissel, M. Hellstrom, K. L. Jones, J. V. Kratz, R. Kulesa, C. Nociforo, R. Palit, H. Simon, G. Surowka, K. Summerer, D. Vretenar, and W. Walus, *Phys. Rev. C* **76**, 051603(R) (2007).  
 [7] S. Abrahamyan *et al.*, *Phys. Rev. Lett.* **108**, 112502 (2012).  
 [8] O. Moreno, P. Sarriguren, E. Moya de Guerra, J. M. Udias, T. W. Donnelly, and I. Sick, *Nucl. Phys. A* **828**, 306 (2009).  
 [9] C. Mondal, B. K. Agrawal, M. Centelles, G. Colò, X. Roca-Maza, N. Paar, X. Viñas, S. K. Singh, and S. K. Patra, *Phys. Rev. C* **93**, 064303 (2016).  
 [10] Z. H. Li, U. Lombardo, H.-J. Schulze, W. Zuo, L. W. Chen, and H. R. Ma, *Phys. Rev. C* **74**, 047304 (2006).  
 [11] J. Piekarewicz and M. Centelles, *Phys. Rev. C* **79**, 054311 (2009).

- [12] I. Vidaña, C. Providência, A. Polls, and A. Rios, *Phys. Rev. C* **80**, 045806 (2009).
- [13] F. Sammarruca and P. Liu, *Phys. Rev. C* **79**, 057301 (2009).
- [14] P. Danielewicz, [arXiv:1003.4011](https://arxiv.org/abs/1003.4011).
- [15] W. D. Myers and W. J. Swiatecki, *Nucl. Phys. A* **81**, 1 (1966).
- [16] P. Möller *et al.*, *At. Data Nucl. Data Tables* **59**, 185 (1995).
- [17] K. Pomorski and J. Dudek, *Phys. Rev. C* **67**, 044316 (2003).
- [18] A. Carbone, G. Colò, A. Bracco, L.-G. Cao, P. F. Bortignon, F. Camera, and O. Wieland, *Phys. Rev. C* **81**, 041301(R) (2010).
- [19] D. Vretenar, T. Nikšić, and P. Ring, *Phys. Rev. C* **68**, 024310 (2003).
- [20] L.-W. Chen, C. M. Ko, and B.-A. Li, *Phys. Rev. C* **72**, 064309 (2005).
- [21] S. Yoshida and H. Sagawa, *Phys. Rev. C* **73**, 044320 (2006).
- [22] L.-W. Chen, C. M. Ko, B.-A. Li, and J. Xu, *Phys. Rev. C* **82**, 024321 (2010).
- [23] C.-H. Lee, T. T. S. Kuo, G. Q. Li, and G. E. Brown, *Phys. Rev. C* **57**, 3488 (1998).
- [24] B. K. Agrawal, *Phys. Rev. C* **81**, 034323 (2010).
- [25] M. K. Gaidarov, A. N. Antonov, P. Sarriguren, and E. Moya de Guerra, *Phys. Rev. C* **84**, 034316 (2011).
- [26] M. K. Gaidarov, A. N. Antonov, P. Sarriguren, and E. Moya de Guerra, *Phys. Rev. C* **85**, 064319 (2012).
- [27] K. A. Brueckner, J. R. Buchler, S. Jorna, and R. J. Lombard, *Phys. Rev.* **171**, 1188 (1968).
- [28] K. A. Brueckner, J. R. Buchler, R. C. Clark, and R. J. Lombard, *Phys. Rev.* **181**, 1543 (1969).
- [29] A. N. Antonov, V. A. Nikolaev, and I. Zh. Petkov, *Bulg. J. Phys.* **6**, 151 (1979); *Z. Phys. A* **297**, 257 (1980); **304**, 239 (1982); *Nuovo Cimento A* **86**, 23 (1985); A. N. Antonov *et al.*, *ibid.* **102**, 1701 (1989); A. N. Antonov, D. N. Kadrev, and P. E. Hodgson, *Phys. Rev. C* **50**, 164 (1994).
- [30] A. N. Antonov, P. E. Hodgson, and I. Zh. Petkov, *Nucleon Momentum and Density Distributions in Nuclei* (Clarendon Press, Oxford, 1988); *Nucleon Correlations in Nuclei* (Springer-Verlag, Berlin, 1993).
- [31] J. J. Griffin and J. A. Wheeler, *Phys. Rev.* **108**, 311 (1957).
- [32] D. Vautherin, *Phys. Rev. C* **7**, 296 (1973).
- [33] E. Moya de Guerra, P. Sarriguren, J. A. Caballero, M. Casas, and D. W. L. Sprung, *Nucl. Phys. A* **529**, 68 (1991).
- [34] E. Feenberg, *Rev. Mod. Phys.* **19**, 239 (1947).
- [35] A. G. W. Cameron, *Can. J. Phys.* **35**, 1021 (1957).
- [36] H. A. Bethe, *Theory of Nuclear Matter*, Annual Review of Nuclear Science, Vol. 21 (Annual Reviews, Palo Alto, 1971), pp. 93–244, Chap. 9.
- [37] Alex E. S. Green, *Rev. Mod. Phys.* **30**, 569 (1958).
- [38] M. Warda, X. Viñas, X. Roca-Maza, and M. Centelles, *Phys. Rev. C* **81**, 054309 (2010).
- [39] M. Centelles, X. Roca-Maza, X. Viñas, and M. Warda, *Phys. Rev. C* **82**, 054314 (2010).
- [40] P. Danielewicz, *Nucl. Phys. A* **727**, 233 (2003).
- [41] P. Danielewicz, [arXiv:nucl-th/0411115](https://arxiv.org/abs/nucl-th/0411115).
- [42] P. Danielewicz and J. Lee, *Nucl. Phys. A* **922**, 1 (2014), and references therein.
- [43] P. Danielewicz and J. Lee, *Int. J. Mod. Phys. E* **18**, 892 (2009).
- [44] P. Danielewicz and J. Lee, *AIP Conf. Proc.* **1423**, 29 (2012), [arXiv:1111.0326](https://arxiv.org/abs/1111.0326) [nucl-th].
- [45] M. B. Tsang, J. R. Stone, F. Camera, P. Danielewicz, S. Gandolfi, K. Hebeler, C. J. Horowitz, Jenny Lee, W. G. Lynch, Z. Kohley, R. Lemmon, P. Möller, T. Murakami, S. Riordan, X. Roca-Maza, F. Sammarruca, A. W. Steiner, I. Vidaña, and S. J. Yennello, *Phys. Rev. C* **86**, 015803 (2012).
- [46] M. B. Tsang, Yingxun Zhang, P. Danielewicz, M. Famiano, Zhuxia Li, W. G. Lynch, and A. W. Steiner, *Phys. Rev. Lett.* **102**, 122701 (2009); M. B. Tsang *et al.*, *Int. J. Mod. Phys. E* **19**, 1631 (2010).
- [47] Akira Ono, P. Danielewicz, W. A. Friedman, W. G. Lynch, and M. B. Tsang, *Phys. Rev. C* **70**, 041604(R) (2004).
- [48] P. Danielewicz, [arXiv:nucl-th/0607030](https://arxiv.org/abs/nucl-th/0607030).
- [49] A. W. Steiner, M. Prakash, J. M. Lattimer, and P. J. Ellis, *Phys. Rep.* **411**, 325 (2005).
- [50] P. Danielewicz and J. Lee, *Nucl. Phys. A* **818**, 36 (2009).
- [51] A. E. L. Dieperink and P. Van Isacker, *Eur. Phys. J. A* **32**, 11 (2007).
- [52] V. M. Kolomietz and A. I. Sanzhur, *Eur. Phys. J. A* **38**, 345 (2008); *Phys. Rev. C* **81**, 024324 (2010).
- [53] N. Nikolov, N. Schunck, W. Nazarewicz, M. Bender, and J. Pei, *Phys. Rev. C* **83**, 034305 (2011).
- [54] S. J. Lee and A. Z. Mekjian, *Phys. Rev. C* **82**, 064319 (2010).
- [55] B. K. Agrawal, J. N. De, S. K. Samaddar, M. Centelles, and X. Viñas, *Eur. Phys. J. A* **50**, 19 (2014).
- [56] M. K. Gaidarov, P. Sarriguren, A. N. Antonov, and E. Moya de Guerra, *Phys. Rev. C* **89**, 064301 (2014).
- [57] W. D. Myers and W. J. Swiatecki, *Ann. Phys. (N.Y.)* **55**, 395 (1969).
- [58] E. Lipparini and S. Stringari, *Phys. Lett. B* **112**, 421 (1982).
- [59] H. Jiang, G. J. Fu, Y. M. Zhao, and A. Arima, *Phys. Rev. C* **85**, 024301 (2012).
- [60] P.-G. Reinhard, M. Bender, W. Nazarewicz, and T. Vertse, *Phys. Rev. C* **73**, 014309 (2006).
- [61] P. Sarriguren, M. K. Gaidarov, E. M. de Guerra, and A. N. Antonov, *Phys. Rev. C* **76**, 044322 (2007).
- [62] G. Audi, A. H. Wapstra, and C. Thibault, *Nucl. Phys. A* **729**, 337 (2003).
- [63] H. v. Groote, E. R. Hilf, and K. Takahashi, *At. Data Nucl. Data Tables* **17**, 418 (1976).
- [64] H. Koura, T. Tachibana, M. Uno, and M. Yamada, *Prog. Theor. Phys.* **113**, 305 (2005).
- [65] A. Ayachi, M. Durand, P. Schuck, and V. S. Ramamurthy, *Z. Phys. A* **327**, 141 (1987).
- [66] N. Sandulescu, P. Schuck, and X. Viñas, *Phys. Rev. C* **71**, 054303 (2005).
- [67] C. Reiß, M. Bender, and P.-G. Reinhard, *Eur. Phys. J. A* **6**, 157 (1999).
- [68] H. Nakada and K. Sugiura, *Prog. Theor. Exp. Phys.* **2014**, 033D02 (2014).
- [69] E. Chabanat, P. Bonche, P. Haensel, J. Meyer, and R. Schaeffer, *Nucl. Phys. A* **635**, 231 (1998); M. Beiner, H. Flocard, N. Van Giai, and P. Quentin, *ibid.* **238**, 29 (1975); N. Van Giai and H. Sagawa, *Phys. Lett. B* **106**, 379 (1981).
- [70] N. Wang, M. Liu, L. Ou, and Y. Zhang, *Phys. Lett. B* **751**, 553 (2015).
- [71] M. Baldo, L. M. Robledo, P. Schuck, and X. Viñas, *Phys. Rev. C* **87**, 064305 (2013).